ASPHERICITY AND TIME VARIATION OF THE NEAR-SURFACE LAYERS OF THE SUN

Sarbani Basu[1], **H. M. Antia**[2], **and Richard S. Bogart**[3]

[1]*Astronomy Department, Yale university, P.O. box 208101, new Haven CT 06520-8101, U. S. A.*
[2]*Tata Institute of Fundamental Research, Homi Bhabha Road, Mumbai 400005, India*
[3]*CSSA-HEPL, Stanford University, Stanford, CA 94305-4085, U. S. A.*

ABSTRACT

We present results on the structure of the near-surface layers of the Sun obtained by inverting frequencies of high-degree solar modes from "ring diagrams". We find that there is a substantial latitudinal variation of both sound speed and the adiabatic index Γ_1 in the outer 2% of the Sun. We find that both the sound-speed and Γ_1 profiles change with changes in the level of solar activity.

Key words: Sun: oscillations; Sun: interior.

1. INTRODUCTION

The mean frequencies of the global modes generally used in helioseismic studies only give the spherically symmetric part of the structure. Departures from spherical symmetry can be studied using even-order splitting coefficients (e.g., Antia *et al.* 2001; Basu & Antia 2003). These results are however, restricted to the deeper layers of the Sun ($r < 0.95R_\odot$) because of the mode sets used. In addition, these studies only yield the azimuthally averaged latitudinal variations in the solar structure. It was found that the sound speed is lower at the equator as compared to higher latitudes. Further, no significant temporal variation was found in deeper layers, while the surface term shows a distinct change with time, implying that there could be changes in the structure closer to the solar surface. The surface term also shows a distinct correlation with the distribution of magnetic fields at the solar surface, which leads us to the conclusion that if we had high degree modes we should be able to detect changes in the structure of the outer layers of the Sun as magnetic activity of the Sun changes.

Since global high degree modes are not available from either the GONG or MDI projects, we use a ring diagram analysis to obtain solar oscillation frequencies of different latitudinal bands of the Sun for different times. We use these frequencies to determine the difference in structure between the equator and the higher latitudes for several epochs covering different activity levels of the Sun.

Table 1. Data sets used

Carrington Rotation	Dates	10.7 cm Flux (SFU)[1]
1910	1996:06:01 – 1996:06:28	71.7 ± 0.3
1922	1997:04:24 – 1997:05:22	74.3 ± 0.6
1932	1988:01:22 – 1998:02:18	87.9 ± 1.5
1948	1999:04:04 – 1999:05:01	120.4 ± 2.5
1964	2000:06:13 – 2000:07:10	188.9 ± 3.8
1975	2001:04:09 – 2001:05:06	169.9 ± 4.6
1988	2002:03:30 – 2002:04:26	196.6 ± 3.1
2009	2003:10:18 – 2003:11:15	159.9 ± 12.1

[1] The errors are $\sigma/\sqrt{(N)}$, σ being the standard deviation of the flux over the observed period, and N the number of days over which the daily 10.7 cm flux is averaged.

2. DATA AND TECHNIQUE

We have analyzed MDI Doppler data from eight complete Carrington rotations contained in the MDI Dynamics campaigns of continuous full-disk resolution coverage. These are listed in Table 1. Also listed is the average flux of 10.7 cm radiation during each period of analysis. The data were untracked in the sense that longitudes were referred to the central meridian of epoch, but corrections were made for the drift of the spacecraft in heliographic latitude in the course of the observing periods. The analysis interval in each case was 39,936 minutes (24×1664 min) covering most of the Carrington rotation.

The highly elliptical ring spectra were fit using the same 13-parameter fit we have used for tracked ring spectra (Basu & Antia 1999), with suitable adjustments for the very large values of the U_x parameter reflecting the advection of the waves by solar rotation. For each Carrington rotation we have thirteen latitude bands of width 15° centred every 7.5° from 45°N to 45°S.

Since magnetic activity is a local phenomena, we have calculated the "Magnetic Activity Index" (MAI) of each

Proc. SOHO 17 – 10 Years of SOHO and Beyond, Giardini Naxos, Sicily, Italy
7 – 12 May 2006 (ESA SP-617, July 2006)

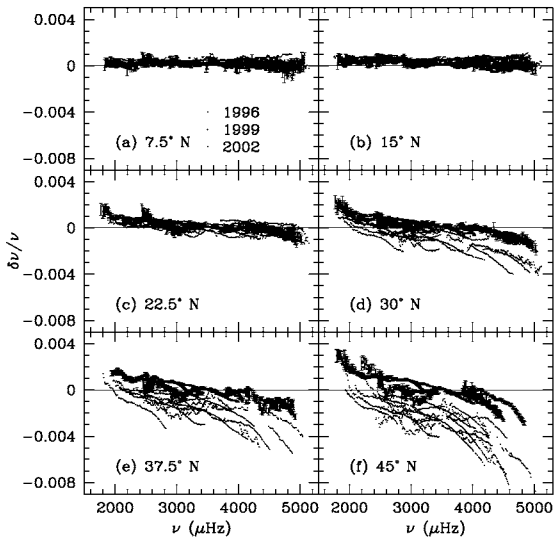

Figure 1. The frequency differences between the higher latitudes and the equator in the northern hemisphere of the Sun for three different epochs. The epochs are labelled by calendar year. The differences are in the sense (Higher latitude − Equator). For the sake of clarity, the error bars are plotted for only one set; they are similar for the other sets.

set to give us a local measure of the magnetic activity which the 10.7 cm radio flux does not. The MAI was calculated by integrating the unsigned field values within the same regions and over the same intervals used to calculate the power spectra, using available 96-minute magnetograms. (See Rajaguru et al. (2001) for more details.)

The differences in structure between two regions of the Sun can be related to the differences in frequencies between the two regions as:

$$\frac{\delta\nu_{n,l}}{\nu_{n,l}} = \int_0^{R_\odot} K^{n,l}_{c^2,\rho}(r)\frac{\delta c^2(r)}{c^2(r)}\,\mathrm{d}r + \int_0^{R_\odot} K^{n,l}_{\rho,c^2}(r)\frac{\delta\rho(r)}{\rho(r)}\,\mathrm{d}r + \frac{F_{\rm surf}(\nu_{n,l})}{I_{n,l}}\,, \quad (1)$$

(e.g., Dziembowski et al. 1990; Däppen et al. 1991; Antia & Basu 1994; Dziembowski et al. 1994, etc.) Here $\delta\nu_{n,l}$ is the difference in the frequency $\nu_{n,l}$ between the two regions, n being the radial order and l the degree. The kernels $K^{n,l}_{c^2,\rho}$ and $K^{n,l}_{\rho,c^2}$ are known functions. Instead of (c^2,ρ), other pairs of functions may be used, such as density and adiabatic index Γ_1. The term involving $F_{\rm surf}$ is the "surface term," which takes into account the near-surface errors in modelling the structure. This term also contains information about the very shallow layers of the Sun that cannot be resolved by the mode-set used.

We use both the Subtractive Optimally Localised Averages (SOLA; Pijpers & Thompson 1992, 1994) and Regularised Least Squares (RLS; Antia 1996) inversion techniques to invert Eq. 1. To eliminate systematic errors in the data caused by changes in plate scale and plate-scale uncertainties we invert the frequency differences between a given latitude and the equator (for the same Carrington rotation) rather than the frequency differences between the different regions and a solar model.

3. RESULTS

Fig. 1 shows the frequency differences between the solar equator and higher latitudes for CR1910(1996), CR1948 (1999) and CR1988 (2002). We can see a distinct difference between 1996 data, which corresponds to a low activity level, and 2002 data which is during a high activity level. The frequency differences are significant in all cases. Similar results are seen for other epochs, and also for the regions in the southern hemisphere. Fig. 2 and 3 show the north-south averaged sound-speed and Γ_1 inversion results. Note that as in the global mode results of Antia et al. (2001), we see that the higher latitudes have higher sound speed than the equator. We also see that Γ_1 is larger at higher latitudes.

Since the surface term from global mode inversions show a correlation with activity, we plot the difference in surface term along with the difference in MAI in Fig. 4. The correlation between the surface term and the δMAI is not very high. The linear correlation coefficient is 0.38 when all data sets are used, but rises to 0.86 when only sets with $|\delta\mathrm{MAI}| > 5$ G are used. The surface term also shows a strong correlation at the higher latitudes with the total activity as measured by the 10.7 cm flux. The correlation coefficient is larger than 0.7 above 30°. The situation at low latitudes is more confused.

In order to better determine the dependence of the results on latitude we concentrate on the averaged results in the radius ranges 0.984–$0.989R_\odot$ and 0.989–$0.994R_\odot$. The averaged results are plotted as a function of latitude in Fig. 4, and as a function of time in Fig. 5. Note that there is a clear latitude dependence, higher latitudes have larger sound-speed and larger Γ_1 as compared to the equator at both radius ranges. The sound-speed decreases closer to the surface. The higher-latitude results show a clear time-dependence. The changes at lower latitudes is smaller. Note that the global-mode results did not show a time dependence, but those results were reliable only up to $0.95R_\odot$. The fact that the global-mode surface term shows a time dependence points to the fact that the structure of layers shallower than $0.95R_\odot$ should show a time dependence, which is indeed what we see.

The averaged sound-speed and Γ_1 differences plotted against the 10.7 cm flux show the dependence of structure on the total activity (see Fig. 6). The correlation is extremely good for the 0.989–$0.994R_\odot$ range, particularly at high latitudes (a absolute value of the correlation coefficient of 0.9 at 45°, the correlation at lower latitudes is weaker). The sound-speed and Γ_1 results show lower correlation with MAI. The linear correlation coefficient between the Γ_1 differences and the MAI differences for the

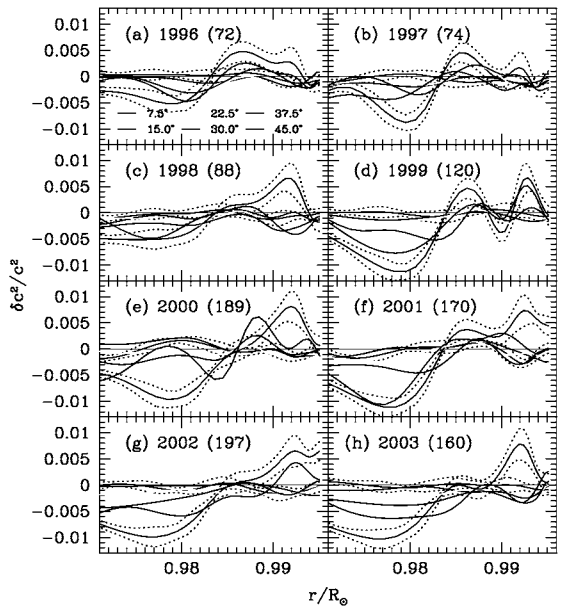

Figure 2. The north-south averaged relative differences in the squared sound speed c^2 between the higher latitudes and the solar equator, plotted as a function of depth for the eight periods analysed. Only RLS results are shown; SOLA results are similar. The dotted lines are 1σ errors. For the sake of clarity, the errors are shown only for latitudes $7.5°$ and $45°$. All differences are in the sense (Higher latitude − Equator). The panels are labelled by the calendar year of the data sets, the numbers in parentheses being the 10.7 cm radio flux in units of SFU for the corresponding period.

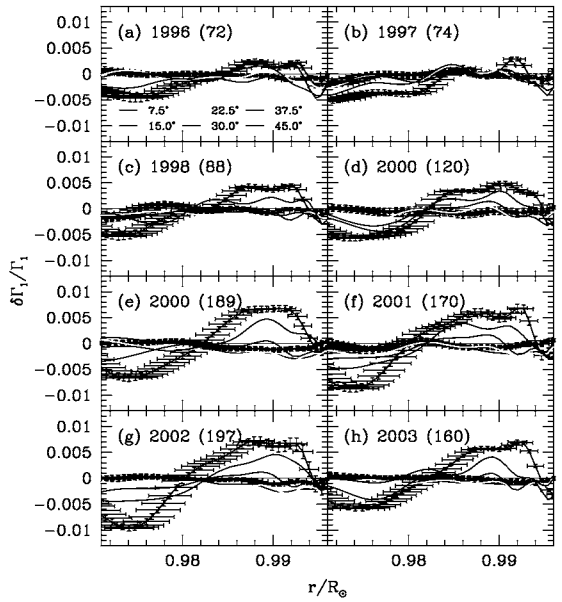

Figure 3. The same as Fig. 2, but for relative differences in Γ_1 and SOLA inversion results.

0.989–$0.994R_\odot$ radius range is only -0.30 for all data sets, but rises to -0.56 if only sets with $|\delta\mathrm{MAI}| > 5$ are included. For sound-speed the correlation coefficients

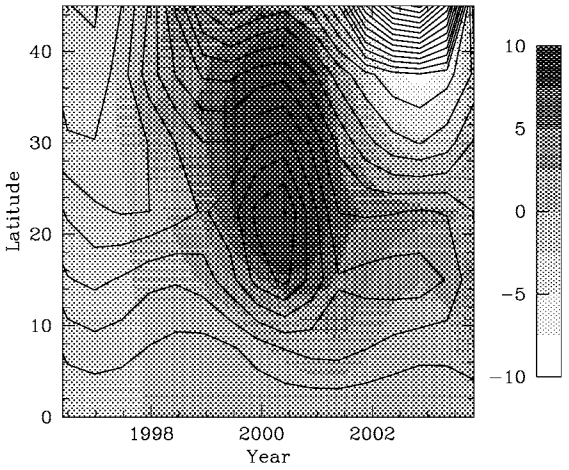

Figure 4. A contour plot of the difference in surface term at 2.5 mHz superposed on a greyscale plot of the δMAI in Gauss. The red contours show positive difference of surface term while blue contours show negative values.

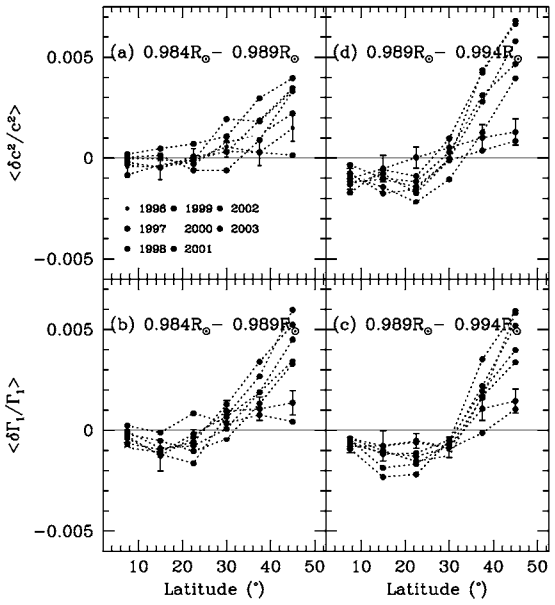

Figure 5. The averaged sound-speed and Γ_1 differences plotted as a function of latitude. Panels (a) & (b) are the averages over the depth range 0.984–$0.989R_\odot$, while panels (c) & (d) are averages over the range 0.989–$0.994R_\odot$. Error bars are shown for the 1996 results; they are comparable for other years. The points are connected to guide the eye.

are smaller (-0.27 and -0.46). This is in seeming contradiction to the results of Basu et al. (2004), but not if we take into account the fact that in that paper, we were dealing with MAI differences that were factor of many

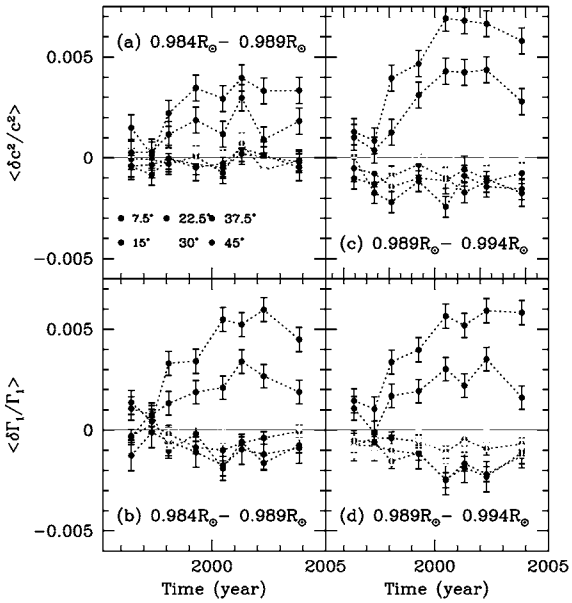

Figure 6. The same as Fig. 5, but plotted as a function of time. Note that the result at a latitude of $30°$ *shows almost no change with time, and latitude* $< 30°$ *and* $> 30°$ *change in the opposite direction. We can therefore infer that the changes in the active-latitudes are different from those at the higher latitudes.*

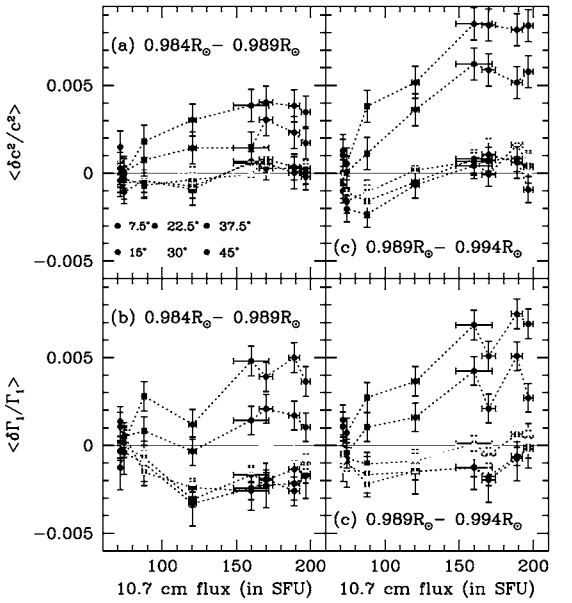

Figure 7. Same as Fig. 5, but plotted as a function of the 10.7 cm radio flux.

(up to 16) larger than the ones in this work, and Basu et al (2004) had seen that the sound-speed and Γ_1 differences do not change much for $|\delta\mathrm{MAI}|$ less than about 30 G. We are dealing with much smaller values here.

4. CONCLUSIONS

There are distinct differences between the near-surface ($0.975R_\odot$ to $0.995R_\odot$) sound speed and Γ_1 profiles between the solar equator and higher latitudes. The differences are largest for latitudes $> 30°$. The surface term has a reasonable correlation with the magnetic activity index (MAI) of the set. The correlation improves if only $|\delta\mathrm{MAI}| > 5$ regions are considered. The sound speed and Γ_1 differences show a time difference and generally tend to increase with increasing activity. The change with time and activity is in opposite directions for latitudes $< 30°$ and latitudes $> 30°$. The correlation coefficients show this too.

ACKNOWLEDGMENTS: This work utilises data from the Solar Oscillations Investigation / Michelson Doppler Imager (SOI/MDI) on the Solar and Heliospheric Observatory (SOHO). SOHO is a project of international cooperation between ESA and NASA. MDI is supported by NASA grant NAG5-8878 to Stanford University. This work is partially supported by NSF grant ATM 0348837 to SB.

REFERENCES

Antia H. M., 1996, A&A 307, 609

Antia H. M., Basu S., 1994, A&AS 107, 421

Antia H. M., Basu S., Hill F., Howe R., Komm R. W., Schou J., 2001, MNRAS 327, 1029

Antia H. M., Basu S., 1994, A&AS 107, 421

Basu S., Antia H. M., 1999, ApJ 525, 517

Basu S., Antia H. M., 2003, in proc. "3D Stellar Evolution Workshop," A.S.P. Conference Series, ASPCS, vol. 293, p. 250

Basu S., Antia H. M., Bogart R. S., 2004, ApJ 610, 1157

Däppen W., Gough D. O., Kosovichev A. G., Thompson M. J., 1991, Lecture notes in Physics, 388, 111

Dziembowski W. A., Pamyatnykh A. A., Sienkiewicz R., 1990, MNRAS 244, 542

Dziembowski W. A., Goode P. R., Pamyatnykh A. A., Sienkiewicz R., 1994, ApJ 432, 417

Pijpers F. P., Thompson M. J., 1992, A&A 262, L33

Pijpers F. P., Thompson M. J., 1994, A&A 281, 231

Rajaguru S. P, Basu S., Antia H. M., 2001, ApJ 563, 410